

X-ray States of Black-Hole Binaries and Implications for the Mechanism of Steady Jets

R. A. Remillard
 MIT Kavli Institute for Astrophysics and Space Research
 Cambridge, MA 02139, USA

RXTE and other high-energy observatories continue to probe the properties of stellar-size black holes and the physics of accretion using bright X-ray transients in the Galaxy. Progress has been made in recognizing that the three states of active accretion are related to different physical elements that may contribute radiation: the accretion disk, a jet, and a compact and radio-quiet corona. Each X-ray state offers potential applications for general relativity in the regime of strong gravity. The temporal evolution of X-ray states is displayed for a few representative black-hole systems. Radio investigations have shown conclusively that the hard X-ray state is associated with the presence of a steady radio jet. The three X-ray states can be synthesized with the “unified model for black hole binary jets” by Fender, Belloni, & Gallo (2004) to gain further insights into the disk:jet connection. The “jet line” appears to coincide with the hard limit of the SPL state. Furthermore there are broad power peaks in PDS that appear to be confined to intermediate and hard states where a jet is present. This suggests that broad power peaks exhibit temporal signatures of non-thermal processes that are related to the jet mechanism, rather than properties inherent to a standard accretion disk.

1. X-ray States of Black Hole Binaries

The X-ray states of black hole binary systems have been re-defined recently in terms of quantitative criteria that utilize both X-ray energy spectra and power density spectra (PDS) [15]. This effort was undertaken in response to the lessons of extensive monitoring campaigns with the *Rossi* X-ray Timing Explorer (*RXTE*), which revealed the full complexity of spectral and timing evolution exhibited by accreting black-hole binary systems [12, 29].

The redefinition of X-ray states uses four criteria: f_{disk} , the ratio of the disk flux to the total flux (both unabsorbed) at 2-20 keV; the power-law photon index (Γ) at energies below any break or cutoff; the integrated rms power (r) in the PDS at 0.1–10 Hz, expressed as a fraction of the average source count rate; and the integrated rms amplitude (a) of a quasi-periodic oscillation (QPO) detected in the range of 0.1–30 Hz. PDS criteria (a and r) utilize a broad energy range, and the bandwidth of the *RXTE* PCA instrument for typical X-ray sources is effectively 2–30 keV.

It had been known for decades that the energy spectra of outbursting black holes often exhibit composite spectra consisting of two broadband components. There is a multi-temperature accretion disk [9, 13, 14, 27] with a characteristic temperature near 1 keV. **Thermal state** designations draw attention to those times when the radiation is dominated by the heat from the inner accretion disk. The thermal state (formerly the “high/soft” state) is defined [15] by the following three conditions: (1) the disk contributes more than 75% of the total unabsorbed flux at 2–20 keV, i.e. $f > 0.75$, (2) there are no QPOs present with integrated amplitude above 0.5% of the mean count rate, i.e. $a_{max} < 0.005$, and (3) the integrated

power continuum is low, with $r < 0.06$.

In principle, the normalization constant for the thermal component may allow numerical estimates of the radius of the inner accretion disk (R_{in}), if the source distance and disk inclination are accurately known [13, 16, 37, 38]. However, such estimates depend on disk models computed under general relativity (GR), with careful attention to the inner disk boundary condition and to effects of radiative transfer [28]. The ongoing efforts to utilize GR disk models and consider all forms of systematic problems in dealing with the inner disk boundary condition may yield reliable measures of R_{in} . This would lead to estimates of the black-hole spin parameter for cases where the black-hole mass is well constrained via measurements of companion star motion in the binary system.

There are other occasions when the spectrum of an outbursting black-hole binary exhibits substantial non-thermal emission in the form of an X-ray power-law component. Observations with *CGRO*–*Ossie* were particularly valuable in showing that there were two types of non-thermal spectra [11], and this perspective has been confirmed with *RXTE*. Spectral fits yield two characteristic values for the photon index. There is a hard state with $\Gamma \sim 1.7$, usually with an exponential decrease beyond ~ 100 keV), and there is a steep power law ($\Gamma \sim 2.5$), with no apparent cutoff. In each case, the corresponding PDS also show distinct differences, relative to the PDS in the thermal state.

The **hard state** has been clearly associated with the presence of a steady type of radio jet [5, 8]. Considerations hard states of for several black-hole binaries allows a definition that is again based on three X-ray conditions: (1) $f < 0.2$, i.e. the power-law contributes at least 80% of the unabsorbed 2–20 keV flux, (2) $1.5 < \Gamma < 2.1$, for a power-law model, cutoff power law, or broken power-law (using Γ_1), as appropriate,

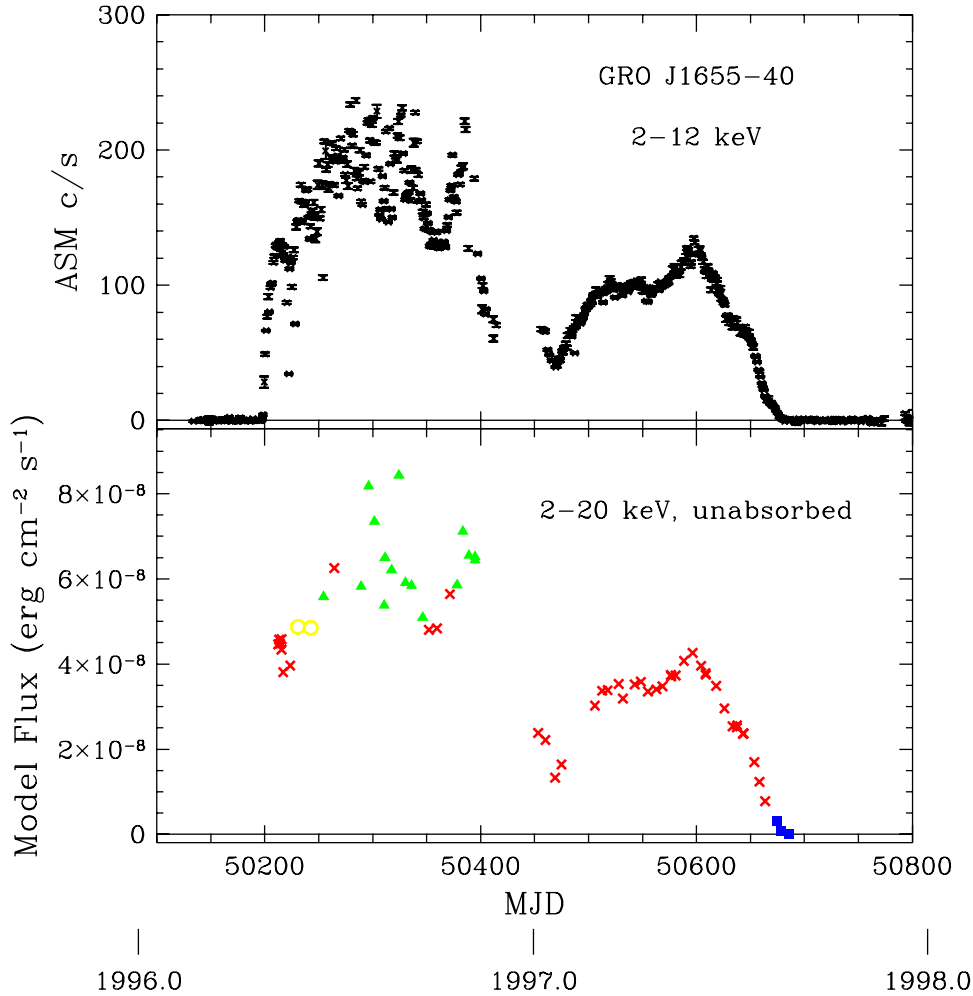


Figure 1: X-ray state evolution during the 1996-1997 outburst of GRO J1655-40. The top panel shows the ASM light curve. The bottom panel shows the model flux from PCA pointed observations. Here the symbol type denotes the X-ray state: thermal (red “x”), hard (blue square), steep power-law (green triangle), and any type of intermediate state (yellow circle).

and (3) the PDS yields $r > 0.1$. In the hard X-ray state, the accretion-disk component is either absent or it is modified in the sense of appearing comparatively cool and large.

The **steep power law** (SPL) state is linked to the strength and properties of the non-thermal spectrum with $\Gamma \sim 2.5$. QPOs are frequently seen when the flux from the SPL begins to compete with thermal component [30]. The SPL state re-defines the “very high” state, which was brought into use when black hole QPOs were first discovered and believed to rare and confined to high luminosity [18, 19]. *CGRO* observations have shown that the SPL may extend to 800 keV or higher [11, 33]. This forces consideration of non-thermal Comptonization models [10, 36]. The

QPOs impose additional requirements for an oscillation mechanism that must be intimately tied to the electron acceleration mechanism, since the QPOs are fairly coherent ($\nu/\Delta\nu \sim 12$; [25]) and strongest above 6 keV, i.e. above the limit of the thermal spectrum, which remains visible during the SPL state. The SPL is further distinguished by its prevalence when high-frequency QPOs are seen (7 sources; 100-450 Hz), and the SPL tends to dominate black-hole binary spectra as the luminosity approaches the Eddington limit [15, 24]. The SPL state is defined by: (1) $\Gamma > 2.4$, (2) $r < 0.15$, and (3) either $f < 0.8$ while a QPO (0.1 to 30 Hz) is present in the PDS (with $a > 0.01$), or $f < 0.5$ with no QPOs.

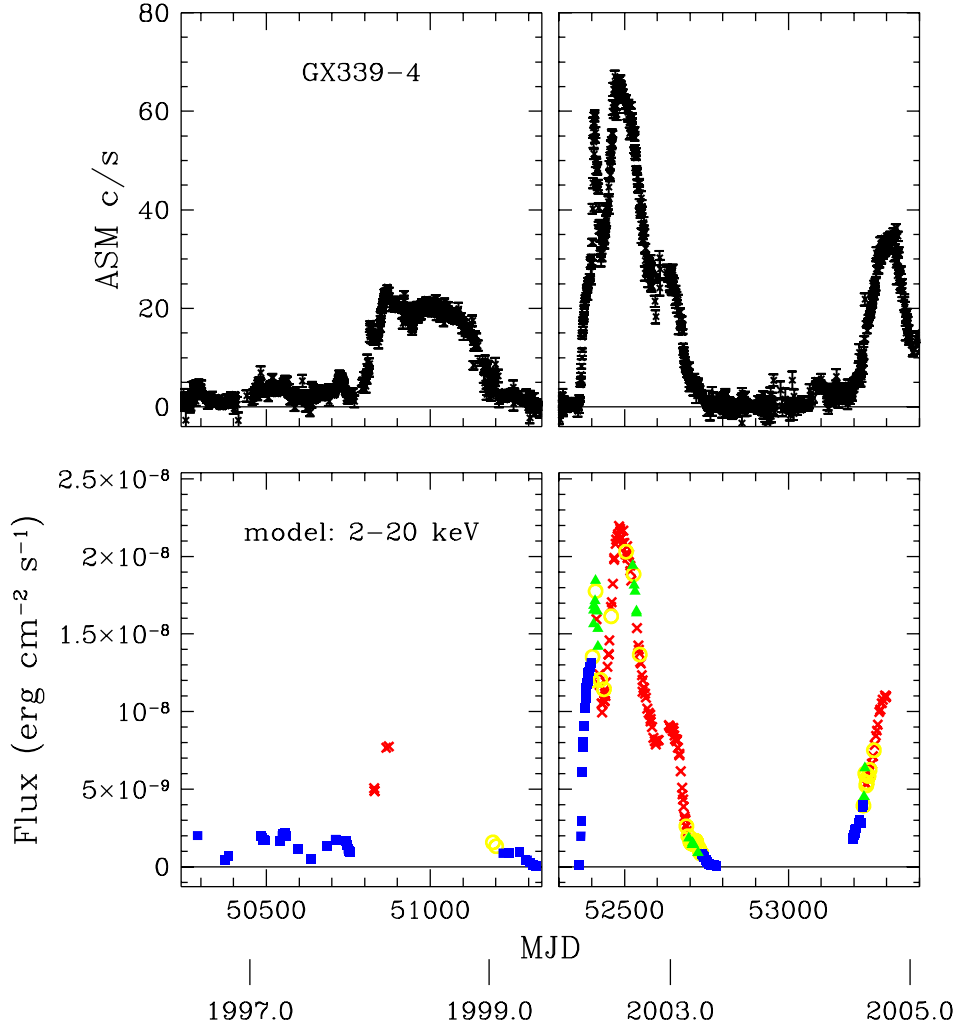


Figure 3: X-ray state evolution during multiple outburst of GX339-4. The top panel shows the ASM light curve. The bottom panel shows the model flux from PCA pointed observations, again using the symbol type to denote the X-ray state, as defined for Fig. 1. GX339-4 was in a quiescent state during 2000 and 2001.

XTE J1550-564 (1998-1999 outburst) is shown in Fig. 2, using the same format and X-ray state representations as in Fig. 1. For this source, spectral modeling efforts follow Sobczak et al. [31], except that a broken power law model is used when it improves the fit significantly, and this happens frequently for observations before MJD 51140. This outburst exhibits several state transitions, and the thermal state is the most common condition (106 cases). The SPL state (30 cases) is again seen when the source reaches highest luminosity; however, the distribution in luminosity is broad (green triangles, Fig. 2). All three states are seen in the range of $1-4 \times 10^{-8} \text{ erg cm}^{-2} \text{ s}^{-1}$. There are many observations (60) of intermediate conditions (yellow circles) during this outburst. Those in the MJD range 51078-51113 display values for the photon

index and rms power that lie between the SPL and hard states (see [15] for more detailed discussions), and they coincide with the appearance of “C” type QPOs that vary substantially in frequency ((0.1-10 Hz) [25]). Near MJD 51300 there is a different group of intermediate cases that lie between the thermal and hard states; they show a hard photon index but there are elevated values of f contributed by the decaying thermal component. This 1998-1999 outburst of XTE J1550-564 was followed by successively weaker outbursts (not shown) in 2000, 2001, 2002, and 2003. The outburst of 2000 again shows multi-state spectral evolution, but the three subsequent and weaker outbursts appear entirely constrained to the hard state (see below).

GX339-4 is chosen as a third example to display

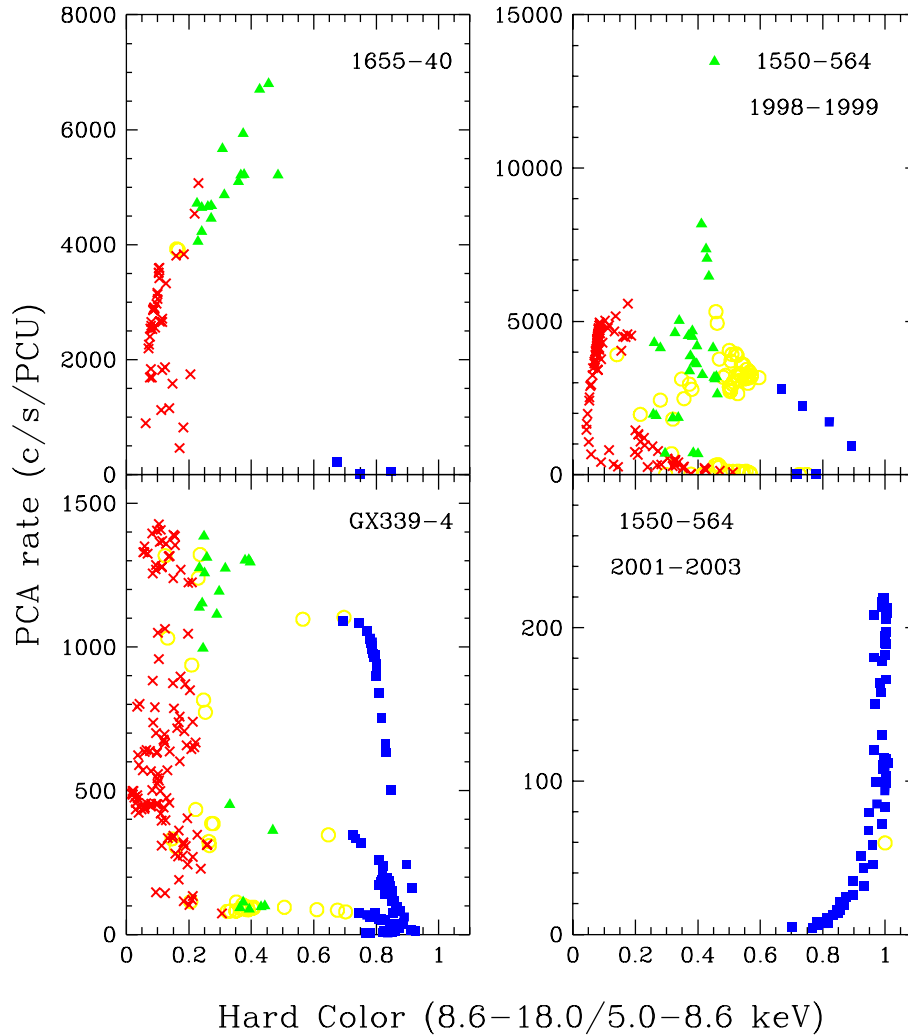


Figure 4: X-ray states displayed on the hardness-intensity diagram. The top-left panel shows GRO J1655-40 results that correspond with the light curve shown in Fig. 1. Also shown are the results for the 1998-1999 outburst of XTE J1550-564 (top-right; see Fig. 2), and all of the observations of GX339-4 (bottom-left; see Fig. 3). The bottom-right panel shows the superposition of three fainter outbursts from XTE J1550-564 to illustrate the point that some outbursts are confined to the hard state.

(see Fig. 3) the temporal evolution of X-ray states in a black-hole binary system. This source is particularly interesting for two reasons: the relatively high accretion rate from the companion star produces frequent X-ray outbursts, and the source is known for extended hard-state episodes, making it a favorite target (along with Cyg X-1) for radio studies and investigations of the disk:jet connection [1, 3, 4, 6, 8, 26]. Three outbursts and a long interval in the hard state (1997) are shown in Fig. 3. GX339-4 was in a quiescent state during 2000 and 2001. All three active X-ray states are represented by GX339-4: 123 thermal states, 95 hard states, 19 SPLs, and 37 that are intermediate.

3. The Unified Model for Radio Jets

Many researchers choose to investigate the spectral evolution of accreting black holes in terms of a hardness-intensity diagrams (HID), where changes in X-ray brightness are tracked vs. a simple “hardness ratio”, i.e. the ratio of detector counts in two energy bands [12, 34]. The HID is also the format chosen for the “unified model for radio jets” proposed by Fender, Belloni, & Gallo [7].

Having defined the X-ray states and their temporal evolution for GRO J1655-40, XTE J1550-564, and GX339-4 in the preceding figures, we now display these same results as HID. These data occupy three

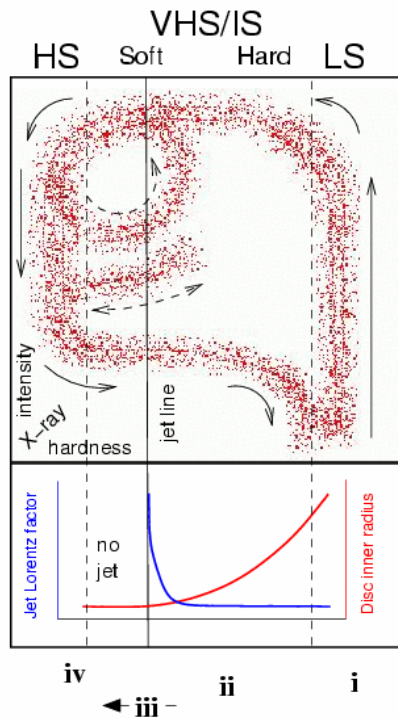


Figure 5: A schematic of the model for disk-jet coupling in black hole binaries from Fender, Belloni, & Gallo (2004). The top panel represents an X-ray HID; the bottom panel illustrates variations in the jet’s bulk Lorentz factor vs. X-ray spectral hardness. The X-ray states are labelled at the top using the older terminology: “high/soft” (HS; “thermal state” in this paper) and “low/hard” (LS; “hard state” here). The “very high/intermediate” state (VHS/IS) in this schematic is resolved into the “SPL” and different types of intermediate states in the definitions of McClintock & Remillard (2005).

of the four panels of Fig. 4. The horizontal scale of this plot utilizes the hard color (HC) defined by Muno, Remillard, & Chakrabarty [20] with a normalization scheme that compensates for PCA gain adjustments and detector evolution that occur during the *RXTE* mission. PCA spectra of the Crab Nebula yield values at $HC = 0.68$, with a normalized intensity of $2500 \text{ c s}^{-1} \text{ PCU}^{-1}$. In Fig. 4, each observation is plotted in the HID with a symbol type and color that shows the X-ray state, using the same conventions of earlier figures.

The fourth panel (bottom-right) of Fig. 4 shows a superposition of color:intensity:state results for XTE J1550-564 during the three weak outbursts noted in §2. For this one panel, there is a slight change in the definition of the hard state. The lower limit for the spectral index is shifted by 0.1, allowing $1.4 < \Gamma < 2.1$, while keeping other criteria the same. This modification is needed to avoid an artificial exclusion of about

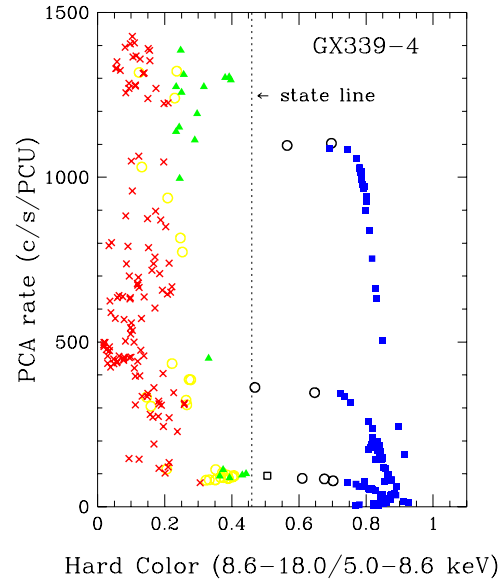


Figure 6: The HID of GX339-4, re-displayed after sorting out the intermediate states into three groups: thermal-SPL intermediates (29 yellow circles), hard-SPL intermediates (7 black circles), and hard-thermal (1 black open square). The dashed line shows the hardness limit for the SPL state in GX339-4, $HC = 0.46$, and this line is hypothesized to coincide with the jet line in the schematic for the unified model of radio jets (Fig. 5). Similar HC limits for the SPL states of GRO J1655-40 and XTE J1550-564 are evident in Fig. 4.

half of these observations ($HC > 0.98$) from the hard state.

Fig. 4 again shows that some outbursts can be dominated by thermal and SPL states (e.g. GRO J1655-40, and additional sources, such as 4U 1543-47 and XTE J2012+381). On the other hand, some outbursts (XTE J1550-564 2001-2003, and also XTE 1118+480 and GS 1324-64) are locked in the hard state. Complex, multi-state outbursts are seen in XTE J1550-564 (1998 and 2000), GX339-4, and sources such as XTE J1859+226, 4U 1630-47, and H1743-322.

We wish to compare these state-represented HID with the ‘unified model for jets’ [7]. The schematic representation of this model is reproduced here for convenience, and further discussions by Fender are available in these proceedings.

GX339-4 obviously plays an important role in shaping the dynamics illustrated in the unified model for jets. However, as recognized by the authors[7], and as shown in Fig. 4, a black hole binary in a given outburst may follow a track that may be more restricted or more complicated than the tracks shown in the model.

The schematic for the disk-jet connection describes not only the flow of states (in the older state conventions), but it also specifies a “jet line” (vertical, solid line center-left in HID of Fig. 5). The jet line represents the boundary between the presence and absence of a steady radio jet, and it also marks a line of conditions where ballistic ejections are most probable. Can such a vertical line be recognized in terms of the revised definitions of X-ray states? The answer appears to be ‘yes’. Corbel et al. [4] have investigated the radio properties of some SPL and intermediate-state observations of XTE J1650-500 and other sources and suggest that the jet terminates at the boundary between the intermediate state and the SPL. In Fig. 4, this transition is shown to have a distinct location on the HID, as the maximum HC value for the SPL state is in the range 0.45–0.48 for each of the three black-hole binary systems. We support the suggestion that this state transition line corresponds to the jet line and encourage further studies with X-ray and radio data for many sources.

The hypothesis that the hard end of the SPL state represents the jet line is illustrated in Fig. 6. Here, the data for GX339-4 (bottom-left panel of Fig. 4) is redisplayed with two changes. The 37 intermediate designations are resolved into 3 groups, to best describe the nearest two states for a given case. There are 29 observations with properties that lie between the thermal and SPL states. They continue to be plotted as yellow circles in Fig. 6. All of these have photon index $\Gamma > 2.4$; fifteen have thermal-like values of r but exhibit either weak QPOs or relatively low values of f ; fourteen have SPL-like values of r and f , but there are no QPOs (although some have broad power features in their PDS). The second group (7 cases) appear to be intermediate between the hard and SPL states, since they have low f values (i.e. nonthermal spectra) with $2.1 < \Gamma < 2.4$ (i.e. photon indices between the hard and SPL states). This group is plotted with black circles in Fig. 6. The single, remaining case is considered to be intermediate between hard and thermal states, since $\Gamma < 2.1$ but $f = 0.34$; this is plotted with a black open square.

The effort to synthesize our definitions of X-ray states with the schematic model for radio jets is encouraging. The identity of the SPL state and the distinctions between different types of intermediate states are well preserved on the HIDs. However, no new insights have been gained, thus far, that are directly pertinent to our understanding of the jet mechanism. Such interests can be served by studying the parameters that define X-ray states in greater detail.

4. X-ray Parameters vs. Hard Color: Implications for Jets

There are three continuous X-ray parameters (apart from “presence of QPOs”) that are used to define X-ray states [15]. These are plotted vs. hard color in Fig. 7 to further investigate how X-ray properties vary across state transitions and across any hypothetical jet line. The symbol choice represents the X-ray state, as defined for Fig. 6.

As one proceeds from right to left in Fig. 7 (i.e. jet “on” towards jet “off”), there do appear to be substantial changes in both the photon index (top panel) and the rms power continuum (bottom panel) at the point where the intermediate (hard/SPL) conditions shift into the SPL state ($HC \sim 0.46$). The disk fraction in the 2–20 keV band (middle panel) appears to be a more continuous function of HC , and the X-ray appearance of the disk above 2 keV begins where the hard state (blue squares) transitions to hard–SPL intermediate conditions (black circles).

The disappearance of the steady radio jet during “hard to soft” X-ray spectral transitions is well known [3, 5, 6], and the behavior of the photon index (top panel of Fig. 7) does suggest that this occurs near $HC \sim 0.46$. However, less attention has been paid to changes in the power spectrum across this transition. The integrated power in the PDS (bottom panel of Fig. 7) is clearly correlated with the value of HC and the X-ray state. What is potentially most interesting about this relationship is the frequency composition of the excess power that follows the evolution of the source in and out of the hard state.

Representative, average PDS were computed for the different states of GX339-4 using 72 thermal-state observations with $0.10 < HC < 0.24$ and 17 SPL observations with $0.24 < HC < 0.45$. For the intermediate and hard states, we find PDS maxima that are a function of brightness, and there are low-frequency QPOs in some of the brighter hard states. These topics need to be investigated further. For the present purpose of illustrating state-specific PDS in GX339-4, we select intermediate and hard-state observations with lower X-ray intensity, $25\text{--}100 \text{ c s}^{-1} \text{ PCU}^{-1}$, to limit the secular variations with brightness and to represent these states at luminosity levels typically seen in other sources. Within these brightness limits, we select 6 intermediate states with $0.50 < HC < 0.72$ and 26 hard states with $0.75 < HC < 0.90$. The PDS (weighted averages) for the four states are displayed in Fig. 8.

In the SPL state, there is a QPO near 5.8 Hz ($a = 0.03$ in the full PCA band), with another peak ($a_2 = 0.01$) at the first harmonic. Note, however, that the average SPL results smear over QPOs with different amplitudes and frequencies, which are better investigated using individual SPL observations.

The PDS for the intermediate (SPL/hard) and hard

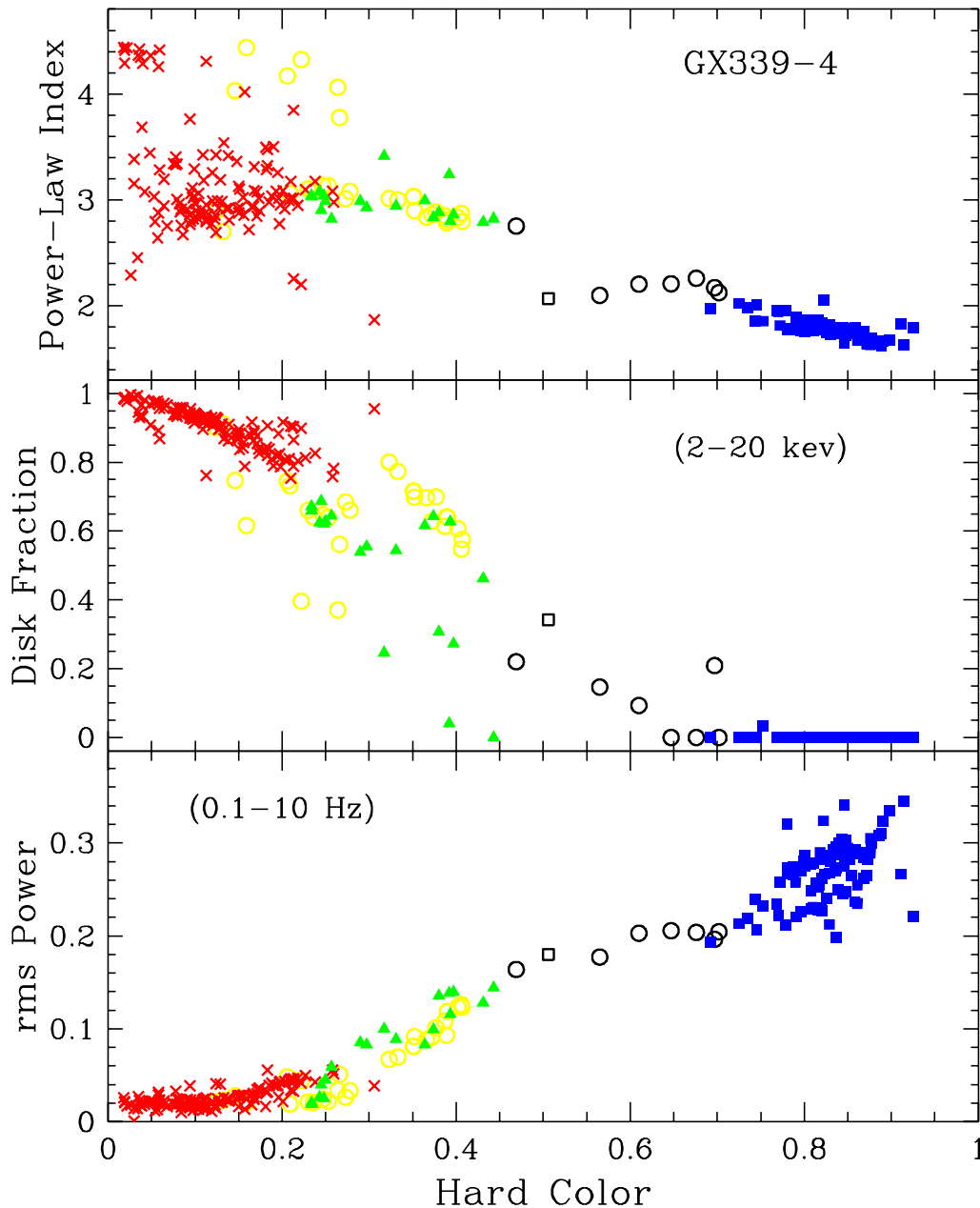


Figure 7: Variations of state-defining parameters vs. hard color for GX339-4. Both the photon index (Γ) and the integrated rms power (0.1–10 Hz) change substantially near $HC \sim 0.46$, supporting the suggestion that this value represents the “jet line”.

states appear quite different; they exhibit broad power peaks [34] with much higher amplitude. These features can be treated as a broad Lorentzian peak superposed on a much broader power continuum, i.e. a quadratic function in $\log(P_\nu)$ vs. $\log(\nu)$ with a fit range of 0.01–1000 Hz. With this type of PDS model, the intermediate (SPL/hard) state yields a broad

power peak that is centered at $\nu_0 = 0.53$ Hz with very low coherence parameter: $Q = \nu_0/FWHM \sim 0.1$. Most of the PDS power ($r \sim 0.2$) is taken up in this broad feature. The hard state PDS can be interpreted with a stronger broad peak centered near 0.2 Hz with $Q \sim 0.14$ and $r \sim 0.3$.

X-ray astronomers have been studying PDS with

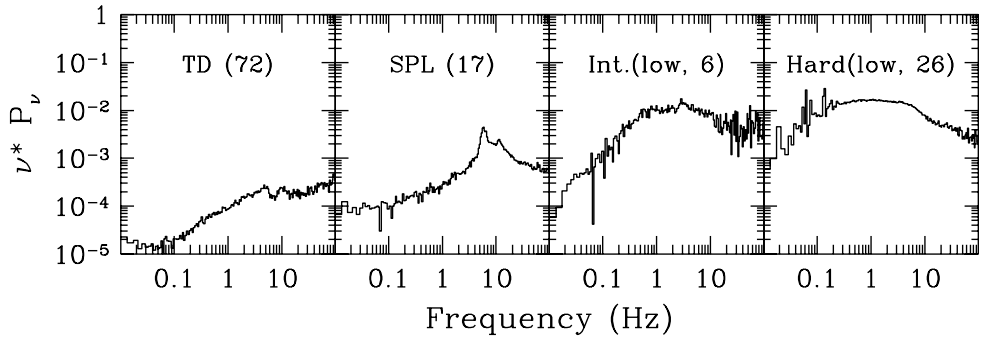


Figure 8: Representative PDS for different X-ray states of GX339-4, displayed in terms of $\log(\nu \times P_\nu)$ vs. $\log(\nu)$. This yields units of $(rms/\mu)^2$ vs. Hz. In each state, the averages are computed for a subset of the observations in a selected range of HC (see text). The broad power peak near 1 Hz is here argued to be an X-ray timing signature associated with the steady radio jet.

“band-limited noise” or broad power peaks in detail for many years [2, 22, 23, 34, 35]. What is perhaps new, here, is the demonstrated need to interpret these features as an X-ray signature that is fundamentally connected to the jet mechanism. These broad power peaks are strongest in the hard state and they seem to form only on the right side of the jet line, i.e. the conditions associated with quasi-steady radio emission.

Pottschmidt et al [22] conducted a detailed analysis of multiple broad peaks with Lorentzian profiles in the PDS of Cyg X-1 in the hard and intermediate states. It was shown that the PDS are best modeled as a superposition of three strong and broad features, e.g near 0.2, 2, and 6 Hz, with correlated variations in frequency and with the occasional presence of a fourth peak near 40 Hz. It was further shown that the stability of the hard state against transitions to intermediate-type flares is related to the strength of the third Lorentzian. These considerations show that the Fourier components related to the hard state are more complicated than the simplified results shown here. However, the point needs to be made that all of these broad power peaks tend to disappear with the hard power-law spectrum when an accreting black hole crosses the jet line.

One can imagine the origin of these broad power peaks in very different ways. In Keplerian terms, the wide range of excess power (i.e. 0.01 to 20 Hz) corresponds to gravitational radii of 30–5000 r_g for a 10 M_\odot black hole with low values of the spin parameter. If some instability at these radii creates the excess PDS power while it furnishes the corona that supplies plasma for the jet, then the base of the jet would be unexpectedly large (0.5 light seconds across the maximum diameter). This picture would seem to be ruled out by the high coherence and ms phase lags measured for Cyg X-1 in the hard and intermediate states (e.g.

[22]).

Since magnetic fields are widely believed to play a central role in the formation of jets in black-hole systems, it may be more productive to consider the PDS power peaks in terms of wave phenomena in a magnetized disk. It has been argued that a vertical magnetic field can excite an “accretion-ejection” instability [32] leading to magnetic spiral waves that may produce both QPOs (at the co-rotation radius for the spiral wave and Keplerian flow in the disk) and Alfvén waves to excite the corona. The broad power peaks in the PDS could be seen as another observational challenge for this model and for MHD simulations of magnetized accretion disks.

Correlations between QPO frequencies and the frequencies associated with broad power peaks have been demonstrated for hard and intermediate state observations of both black-hole binaries and accreting neutron stars [2, 23, 35]. The neutron-star connection naturally motivates the presumption that the behavior of X-ray power peaks is dictated by standard accretion-disk physics. However, the consideration of black-hole hard states and the jet line motivates an alternative viewpoint: the frequency relationships for broad power peaks are primarily exhibiting the behavior of non-thermal processes that are related to the jet mechanism. As a corollary question, we may need to understand why jets appears to be less efficient in the hard states of accreting neutron stars [17, 21].

Acknowledgments

This work was supported by the NASA contract to MIT for the ASM and EDS instruments on *RXTE*. Special thanks are extended to Jeff McClintock for many contributions to this research.

References

- [1] T. Belloni, M. Mendez, M. van der Klis, W. H. G. Lewin, and S. Dieters, *Ap. J.*, **519**, L159–L163 (1999).
- [2] T. Belloni, M. Mendez, D. Psaltis, and M. van der Klis, *Ap. J.*, **572**, 392–406 (2002).
- [3] S. Corbel, et al., *A&A*, **359**, 251–268 (2000).
- [4] S. Corbel, R. Fender, J. A. Tomsick, A. K. Tzioumis, and S. Tingay, *Ap. J.*, **617**, 1272–1283 (2004).
- [5] R. Fender, “Jets from X-ray binaries”, in *Compact Stellar X-ray Sources*, edited by W. H. G. Lewin and M. van der Klis, Cambridge University Press, Cambridge, 2005, in press (astro-ph/0303339).
- [6] R. Fender, et al., *Ap. J.*, **519**, L165–L168 (1999).
- [7] R. Fender, T. M. Belloni, and E. Gallo, *MNRAS*, **355**, 1105–1118 (2004).
- [8] E. Gallo, R. Fender, and G. G. Pooley, *MNRAS*, **344**, 60–72 (2003).
- [9] M. Gierlinski, and C. Done, *MNRAS*, **347**, 885–894 (2004).
- [10] M. Gierlinski, and C. Done, *MNRAS*, **342**, 1083–1092 (2003).
- [11] J. E. Grove, W. N. Johnson, R. A. Kroeger, K. McNaron-Brown, and J. Skibo, *Ap. J.*, **500**, 899–908 (1998).
- [12] J. Homan, et al., *Ap. J. Suppl.*, **132**, 377–402 (2001).
- [13] L.-X. Li, E. R. Zimmerman, R. Narayan, and J. E. McClintock, *Ap. J. Suppl.*, **157**, 335–370 (2005).
- [14] K. Makishima, et al., *Ap. J.*, **308**, 635–643 (1986).
- [15] J. E. McClintock, and R. A. Remillard, “Black Hole Binaries”, in *Compact Stellar X-ray Sources*, edited by W. H. G. Lewin and M. van der Klis, Cambridge University Press, Cambridge, 2005, in press (astro-ph/0306213).
- [16] A. Merloni, A. C. Fabian, and R. R. Ross, *MNRAS*, **313**, 193–197 (2000).
- [17] S. Migliari, R. P. Fender, M. Rupen, P. G. Jonker, M. Klein-Wolt, R. M. Hjellming, and M. van der Klis, *MNRAS*, **342**, L67–L71 (2003).
- [18] S. Miyamoto, S. Iga, S. Kitamoto, and Y. Kamado, *Ap. J.*, **403**, L39–L42 1993.
- [19] S. Miyamoto, and S. Kitamoto, *Ap. J.*, **374**, 741–743 1991.
- [20] M. P. Muno, R. A. Remillard, and D. Chakrabarty, *Ap. J.*, **568**, L35–L39 (2002).
- [21] M. P. Muno, T. Belloni, V. Dhawan, E. H. Morgan, R. A. Remillard, and M. P. Rupen, *Ap. J.*, in press (2005); astro-ph/0411313.
- [22] K. Pottschmidt, et al. *A&A*, **407**, 1039–1058 (2003).
- [23] D. Psaltis, T. Belloni, and M. van der Klis, *Ap. J.*, **520**, 262–270 (1999).
- [24] R. A. Remillard, M. P. Muno, J. E. McClintock, and J. A. Orosz, *Ap. J.*, **580**, 1030–1042 (2002).
- [25] R. A. Remillard, G. J. Sobczak, M. P. Muno, and J. E. McClintock, *Ap. J.*, **564**, 962–973 (2002).
- [26] M. Revnivtsev, M. Gilfanov, and E. Churazov, *A&A*, **380**, 520–525 (2001).
- [27] N. I. Shakura, and R. A. Sunyaev, *A&A*, **24**, 337–366 (1973).
- [28] T. Shimura, and R. Takahara, *Ap. J.*, **445**, 780–788 (1995).
- [29] G. J. Sobczak, J. E. McClintock, R. A. Remillard, C. D. Bailyn, and J. A. Orosz, *Ap. J.*, **520**, 776–787 (1999).
- [30] G. J. Sobczak, et al., *Ap. J.*, **531**, 537–545 (2000).
- [31] G. J. Sobczak, et al., *Ap. J.*, **544**, 993–1015 (2000).
- [32] M. Tagger, and R. Pellat, *A&A*, **349**, 1003–1016 (1999).
- [33] J. A. Tomsick, P. Kaaret, R. A. Kroeger, and R. A. Remillard, *Ap. J.*, **512**, 892–900 (1999).
- [34] M. van der Klis, “A Review of Rapid Variability in X-ray Binaries”, , in *Compact Stellar X-ray Sources*, edited by W. H. G. Lewin and M. van der Klis, Cambridge University Press, Cambridge, 2005, in press (astro-ph/0410551).
- [35] R. Wijnands and M. van der Klis, *Ap. J.*, **514**, 939–944 (1999).
- [36] A. A. Zdziarski, and M. Gierlinski, *PThPS*, **155**, 99–119 (2004).
- [37] S. N. Zhang, W. Cui, and W. Chen, *Ap. J.*, **482**, L155–L158 (1997).
- [38] E. R. Zimmerman, R. Narayan, J. E. McClintock, and J. M. Miller, *Ap. J.*, **618**, 832–844 (2005).